Turbulence and intermittency in the heliospheric magnetic field in fast and slow solar wind

E. Yordanova, A. Balogh, A. Noullez, R. von Steiger

Turbulence and intermittency in the heliospheric magnetic field in fast and slow solar wind

E. Yordanova,[1,2,3] A. Balogh,[1] A. Noullez,[4] and R. von Steiger[1]

Received 13 January 2009; revised 25 April 2009; accepted 27 May 2009; published 1 August 2009.

[1] We study the nonuniform solar wind turbulence using high-resolution Ulysses magnetic field data measured at different solar activity level, heliospheric latitudes, and distance. We define several types of solar wind dependent of the coronal region of origin and also of the dynamical behavior of the different streams, namely, ''pure'' fast wind, fast streams, ''pure'' slow wind, and slow streams. The turbulent properties of the solar wind types were investigated in terms of their scaling properties and spatial inhomogeneity. A clear trend in the power spectrum of the solar wind magnetic field magnitude is observed: the ''pure'' fast wind has a slope ~ -1.33 ($1/f$-like), the fast streams ~ -1.48 (Kraichnan-like), the ''pure'' slow wind ~ -1.67 (Kolmogorov-like), and the slow streams ~ -1.72. We find that the ''pure'' fast wind in the polar heliolatitudes is less intermittent than the other types: ''pure'' slow wind and both slow and fast streams, which is because of the absence of dynamical interactions between streams with different speeds. On the other hand, fast streams are more intermittent than the ''pure'' fast wind, and slow streams are less intermittent than the ''pure'' slow winds. A clear radial and latitudinal evolution of the intermittency is observed only for the ''pure'' fast wind, while in the equatorial plane, the fast streams, the ''pure'' slow wind, and the slow streams do not show evolution either in heliolatitude or in heliocentric distance.

Citation: Yordanova, E., A. Balogh, A. Noullez, and R. von Steiger (2009), Turbulence and intermittency in the heliospheric magnetic field in fast and slow solar wind, *J. Geophys. Res.*, *114*, A08101, doi:10.1029/2009JA014067.

1. Introduction

[2] The solar wind plasma and the heliospheric magnetic field frozen into the flow are described by parameters whose values fluctuate on all timescales. The vector magnetic field fluctuates, usually with higher amplitude fluctuations in its components than in magnitude. The solar wind velocity, density, temperature and composition, also show fluctuations that cannot be described satisfactorily by time-independent statistical parameters.

[3] Solar wind fluctuations have been described in terms of turbulence since the early work of *Coleman* [1968] who found that, in general, the power spectrum of the fluctuations was consistent with a Kolmogorov description of a turbulent fluid which, over a limited frequency or wavelength interval had a slope of $-5/3$. Shortly afterwards, another view of the fluctuations emerged: at least some of the time (when the solar wind speed was high), transverse Alfvén waves were identified by *Belcher and Davis* [1971] as a dominant contributor to the fluctuations. Over the past four decades, a considerable amount of research has described many aspects of solar wind fluctuations in terms of turbulence using many of the concepts, terminology and techniques from fluid turbulence (for reviews, see the works of *Tu and Marsch* [1995], *Goldstein and Roberts* [1999], *Bruno et al.* [2003], and *Bruno and Carbone* [2005]). The persistent and significant deviations of the fluctuations from the homogeneous case of Kolmogorov-like turbulence have been described in terms of intermittency. This concept implies that the fluctuations are not space filling, nor self-similar over a meaningful range of wavenumbers and their distribution departs significantly from a Gaussian. Historically, the intermittency of solar wind fluctuations was identified and described using structure functions (*Burlaga* [1991], *Marsch and Liu* [1993], *Chapman and Hnat* [2007], see also *Horbury and Balogh* [1997], on the limitations of using structure functions). For the identification and analysis of intermittency over a range of conditions in the solar wind, using different techniques, see the works of *Horbury and Balogh* [2001], *Bruno et al.* [2003], *Bruno and Carbone* [2005], and *Kiyani et al.* [2007]. It is generally accepted that fluctuations in the solar wind are always intermittent. It has been found that the levels of intermittency, measured in fluctuations in either solar wind parameters or magnetic field parameters, vary significantly. The variations have been described as a function of high- and low-speed solar wind [*Bavassano et al.*, 1982a; *Horbury and Balogh*, 2001], heliocentric distance [*Bavassano et al.*, 1982a; *Marsch and Tu*, 1990; *Bruno et al.*, 2003] and heliolatitude [*Horbury et al.*, 1996]. The heliolatitude dependence, however, may be

[1]International Space Science Institute, Bern, Switzerland.
[2]Space Plasma Physics, Swedish Institute of Space Physics, Uppsala, Sweden.
[3]Space Physics, Space Research Institute, Sofia, Bulgaria.
[4]Laboratoire Casioppe, Observatoire de Nice, Nice, France.

0148-0227/09/2009JA014067

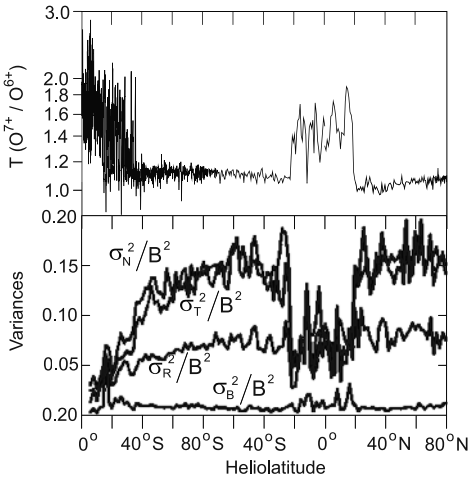

Figure 1. (top) Freezing-in temperature of oxygen ions in the corona as a function of heliolatitude as measured by the SWICS instrument on the Ulysses mission in 1992 to 1996. Low temperatures indicate the origin of the solar wind in the large polar coronal holes, while the higher temperatures are prevalent in the equatorial region where interacting slow and fast winds are present. The boundary between regions of fast and mixed speed wind streams is seen to be very sharp. (bottom) Normalized variances of the magnetic field components and magnitude (b_R/B^2, b_T/B^2, b_N/B^2, and b_B/B^2) B^2) along the solar polar orbit of Ulysses between 1992 and 1996, plotted as a function of heliolatitude. The nature of fluctuations is clearly dependent on the region of origin of the solar wind.

only a composite (and consequence) of dependencies on distance and solar wind regime. The scaling properties of the solar wind kinetic parameters and magnetic field show also solar cycle variation [*Bruno et al.*, 2007a; *Chapman et al.*, 2008; *Podesta et al.*, 2007; *Bavassano et al.*, 2009].

[4] Fluctuations in the solar wind and magnetic field are highly nonuniform and appear to depend on heliospheric conditions, and both on location and on time. Nonuniformity in solar wind speed arises routinely between fast speed streams from coronal holes and slow speed streams from the proximity of closed magnetic fields. In the course of solar wind expansion, because of speed differentials, a fast speed stream following a slow speed stream necessarily interacts with it, forming large Corotating Interaction Regions (CIRs [see *Balogh et al.*, 1999]). In CIRs, the slow wind is speeded up and the fast wind is slowed down, with the density becoming compressed and with an increase in kinetic temperature. In that case, instead of taking velocity as a differentiator between two interacting streams, the distinction is best determined by charge state composition of heavy ions, representing the coronal temperature (in coronal holes, or in solar streamer-like regions) of the source regions of the wind [*Geiss et al.*, 1995; *Wimmer-Schweingruber et al.*, 1997].

[5] The heliolatitude dependence of the magnetic field fluctuations, as measured by the normalized hourly variances in the components and the magnitude of the field, as a function of heliolatitude around the orbit of the Ulysses spacecraft is shown in Figure 1 [from *Forsyth et al.*, 1996]. In the highly uniform high-speed solar wind, magnetic fluctuations are characterized by large, transverse Alfvénic fluctuations and smaller, by a factor ~2, fluctuations in the radial component of the magnetic field. Fluctuations in the magnitude of the magnetic field are even smaller, by another factor ~5. In the equatorial region of mixed, interacting slow- and high-speed streams the variances of the transverse fluctuations drop significantly and become comparable to the variance in the radial component of the field. The variance in the magnetic field magnitude is somewhat more variable and higher than in the uniform high-speed flows; these variations are caused by the compressive effects in CIRs.

[6] The fluctuations are contrasted with the coronal freezing-in temperature measured by the oxygen charge state ratio O^{7+} to O^{6+} in Figure 1 (top). Figure 1 indicates clearly the different character of fluctuations in the polar high-speed streams. In the equatorial regions, the interacting slow- and high-speed streams make the fluctuations in the components of the magnetic field approximately equal.

[7] One way to investigate the turbulent evolution of the heliospheric medium is to study the parameters that characterize the turbulence and the intermittency in different regimes of solar wind flow. The largest levels of dynamic input into the energy transfer process between scales are likely to occur in the regime dominated by CIRs. The flow regime least affected by dynamical evolution is the high-speed solar wind from the large polar coronal holes around solar minimum. The slow solar wind, on the other hand is highly variable in its flow parameters and therefore dynamically active from the time it leaves the corona. Its turbulence parameters show that it is highly evolved by 1 AU [*Bavassano et al.*, 1982b; *Denskat and Neubauer*, 1982] and that it evolves at a decreasing rate beyond 1 AU [*Roberts et al.*, 1987; *Roberts and Goldstein*, 1991].

[8] In this paper we investigate the solar wind turbulence and intermittency with dependence on the heliospheric latitude, heliospheric distance, and solar activity. It is organized as following: in section 2 we present the tools that are used in the study to characterize and visualize the magnetic field turbulence and intermittency, in section 3 we introduce the data sets, we define the different types of solar wind and provide the background information for the measurements, in section 4 the results are described and discussed, and we complete the paper with the conclusions in section 5.

2. Techniques for Characterizing Turbulence and Intermittency

[9] In this study we use classical tools to characterize the statistical properties and intermittency of the magnetic field turbulence on the basis of data samples of different types of solar wind: "pure" fast wind and fast streams, and "pure" slow wind and slow streams (the types are going to be defined further in section 3). We investigate the scaling behavior of the structure functions of the solar wind magnetic fluctuations and their deviation from the theoretical models. We also provide a graphical representation of the distribution of magnetic field fluctuations in space, which gives us an idea about their spatial distribution.

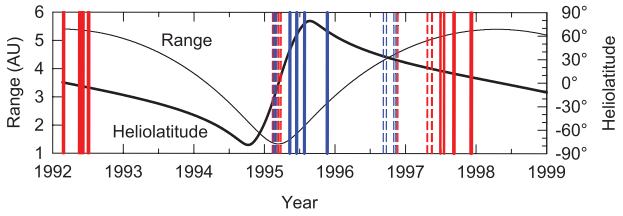

Figure 2. Ulysses orbit as a function of the heliolatitude (the thick black line) and distance from the Sun (the thin black line). The vertical lines mark the periods that have been analyzed. Red solid lines correspond to periods of "pure" slow wind, red dashed lines to slow streams, blue solid lines to "pure" fast, and blue dashed lines to fast streams.

2.1. Flatness and Structure Functions

[10] Fully developed, homogeneous turbulence can be considered as self-similar, that is, at different magnifications the fluctuations of the turbulent media look the same and have the same statistical properties [see *Frisch*, 1995]. The presence of strong bursts of turbulent activity leads to breakdown of the self-similarity. As the timescales become small, these very intensive fluctuations become more and more important and they dominate the statistics. This behavior is attributed to the presence of the intermittency in the fluctuations.

[11] Characterizing the intermittency and estimating its importance for the turbulence dynamics and structure formation remains one of the fundamental problems of the modern physics of plasma and neutral fluid turbulence. The degree of the intermittency can be estimated by calculating of the flatness F (the forth-order normalized structure function) [*Frisch*, 1995].

$$F(\Delta t) = \frac{\langle S^4_{\Delta t} \rangle}{\langle S^2_{\Delta t} \rangle^2}, \qquad (1)$$

where $S^q_{\Delta t} = \langle |g(t + \Delta t) - g(t)|^q \rangle$ is the structure function of order q of the increments of a fluctuating field g (e.g., velocity or magnetic field) separated by a time interval Δt. In the inertial range, where the energy is transferred without preference of scale (scale-invariance), the structure function exhibits a power law behavior: $S^q_{\Delta t} = \Delta t^{\zeta_q}$. For self-similar time series, the exponents of this power law follow a linear relation. In Kolmogorov theory of neutral fluid turbulence $\zeta_q = q/3$, in the magnetohydrodynamic analog (Kraichnan-Iroshnikov) $\zeta_q = q/4$.

2.2. 3-D Representation of the Fluctuations

[12] The behavior of the magnetic field fluctuations can be visualized by plotting the trajectory of the tip of the normalized magnetic field vector in three-dimensional space. The field components plotted versus each other (b_R versus b_T, b_R versus b_N and b_T versus b_N as well as the 3-D projection of the path of the unit vector) illustrate the spatial filling of the magnetic fluctuations in the respective plane projections. This procedure is a convenient way for revealing whether fluctuations are homogeneously distributed in space or not when comparing different solar wind types, keeping in mind that the interplanetary magnetic field is preferentially aligned with the Parker direction. Examples for such distributions of the spatial fluctuations are presented later in the paper.

3. Data Analysis

[13] In this paper we present results from the analysis of data samples from Ulysses magnetic field measurements [*Balogh et al.*, 1992] in the period 1992–1997 (Figure 2). The Ulysses spacecraft was placed into an eccentric, near-polar orbit around the Sun and thus has been able to provide observations of the solar wind and the heliospheric magnetic field as a function of both heliocentric distance and heliolatitude. 1992 marks the beginning of the descending phase of the solar activity cycle 22. Figure 2 also indicates the specific times and heliographic positions of the intervals of observations analyzed in the paper.

3.1. Data Description

[14] We have investigated 21 intervals of different solar wind types. The list of the data samples is given in Table 1, together with the heliospheric latitude and distance from the Sun. The duration of the analyzed periods varies from 2 to 19 days. We have chosen four intervals during a long period of relatively low wind velocity at distances about 5.3–5.4 AU and latitudes 7°–13°S. Further in the paper we will to refer these intervals as "pure" slow solar wind. There was a similar low-speed period in the 1997, close to the minimum of the solar activity, where we have taken for comparison three intervals of "pure" slow wind. At this time Ulysses was at a location similar to the one in 1992: about 5.1–5.3 AU and slightly closer to the solar equator (0°–8°N). During 1994 and 1995 Ulysses moved from the south polar region (80°S) across the equator to the north polar region (80°N) in a trajectory referred as the "fast latitude scan". In 1995, Ulysses was positioned at about 1.5 AU. The solar wind in this period of the scan (20°S–20°N) is a mixture of interacting fast and slow solar wind streams. We have separated several slow and fast streams using the criterion described below in the section 3.2. The same criterion was used to separate slow and fast streams in the 1996 data (at heliospheric distances: 4.3–4.6 AU and heliolatitudes 22°–27°N) and from 1997 (heliospheric distance: 5.0 AU and heliospheric latitude 12°N) in order to increase the number of sampled intervals for comparison. We have also considered time intervals in 1995, during which Ulysses was making measurements in the polar fast wind, which we will call "pure" fast wind. With this large set of data samples in hand we attempt to examine the dependence of the solar wind turbulence on heliolatitude, heliocentric distance, and the level of solar activity. In order to avoid the mixing of different processes and characterize correctly the turbulence in the different solar wind types we analyze periods without coronal mass ejection (CME) occurrences.

3.2. Separation of Slow and Fast Streams

[15] The kinetic parameters (speed, density) of the solar wind are a poor indicator for the type of solar wind. A more reliable criterion would be based on the distribution of charge states of the ions (oxygen) in the solar wind, from which the coronal temperature can be obtained directly. As the solar wind expands outward, the coronal electron

Table 1. Spacecraft Position, Spectral Index and Flatness of the Analyzed Periods

					Spectral Index			Flatness		
Wind Type	Days	Year	Latitude (°)	AU	b_R	b_T	b_N	B	b_R	b_T	b_N
Pure fast	129.0–133.0	1995	50	1.5	1.65 ± 0.02	1.60 ± 0.02	1.62 ± 0.02	1.25 ± 0.02	7.8	7.9	8.3
	165.0–169.0	1995	68	1.7	1.59 ± 0.02	1.66 ± 0.02	1.62 ± 0.02	1.31 ± 0.02	7.9	7.4	8.1
	205.0–209.0	1995	80	2.0	1.64 ± 0.02	1.69 ± 0.02	1.62 ± 0.02	1.37 ± 0.03	9.0	9.1	8.6
	323.0–327.0	1995	60	3.0	1.64 ± 0.02	1.64 ± 0.02	1.69 ± 0.03	1.38 ± 0.02	8.1	8.8	10.6
Fast streams	47.5–49.5	1995	−12	1.4	1.55 ± 0.04	1.60 ± 0.04	1.60 ± 0.05	1.47 ± 0.06	22.6	15.5	13.7
	57.5–60.7	1995	−4	1.4	1.61 ± 0.02	1.65 ± 0.02	1.71 ± 0.03	1.47 ± 0.03	11.2	13.3	12.0
	250.0–266.0	1996	27	4.3	1.69 ± 0.01	1.76 ± 0.01	1.78 ± 0.01	1.52 ± 0.01	16.4	20.5	19.0
	304.0–315.0	1996	23	4.5	1.69 ± 0.02	1.72 ± 0.02	1.79 ± 0.01	1.47 ± 0.02	14.4	15.5	16.0
Pure slow	53.0–58.0	1992	−7	5.4	1.64 ± 0.02	1.58 ± 0.02	1.77 ± 0.01	1.71 ± 0.04	23.3	27.3	32.1
	136.0–144.0	1992	−11	5.4	1.75 ± 0.02	1.81 ± 0.02	1.77 ± 0.01	1.71 ± 0.04	25.5	51.9	23.8
	151.0–159.0	1992	−12	5.4	1.65 ± 0.03	1.62 ± 0.03	1.64 ± 0.02	1.64 ± 0.04	34.0	43.7	21.7
	182.0–188.0	1992	−13	5.3	1.83 ± 0.03	1.74 ± 0.03	1.72 ± 0.03	1.55 ± 0.03	23.1	20.2	19.6
	180.0–199.0	1997	8	5.1	1.68 ± 0.01	1.71 ± 0.01	1.63 ± 0.01	1.76 ± 0.01	23.9	49.3	20.8
	247.0–253.0	1997	5	5.2	1.70 ± 0.02	1.77 ± 0.02	1.75 ± 0.02	1.76 ± 0.03	28.7	38.8	25.1
	336.0–343.0	1997	0	5.3	1.46 ± 0.02	1.45 ± 0.02	1.53 ± 0.01	1.55 ± 0.02	20.7	22.4	20.3
Slow streams	40.6–43.2	1995	−17	1.4	1.73 ± 0.02	1.82 ± 0.02	1.71 ± 0.02	1.78 ± 0.03	17.2	31.2	41.1
	69.0–73.0	1995	6	1.4	1.69 ± 0.03	1.89 ± 0.03	1.71 ± 0.03	1.76 ± 0.02	18.8	20.6	17.3
	80.7–85.4	1995	15	1.4	1.84 ± 0.03	1.88 ± 0.03	1.71 ± 0.03	1.78 ± 0.03	12.1	19.7	11.4
	320.0–325.0	1996	22	4.6	1.78 ± 0.02	1.85 ± 0.02	1.73 ± 0.03	1.68 ± 0.02	19.3	25.4	16.8
	111.0–114.0	1997	12	5.0	1.81 ± 0.03	1.95 ± 0.03	1.67 ± 0.03	1.62 ± 0.03	20.1	33.1	17.0
	134.0–138.0	1997	11	5.0	1.68 ± 0.02	1.74 ± 0.02	1.52 ± 0.02	1.69 ± 0.02	16.5	21.0	11.7

density decreases to the extent that the timescale of coronal expansion is short compared to the ionization and recombination timescale. At a few solar radii in the corona, the relative ionization states become constant (''freeze in''). Thus at any further distance in space, the charged states can be used as proxies for the coronal temperature providing information about the conditions and processes at the sites of the solar wind origins (low corona) and the observing site [*von Steiger et al.*, 2001]. The oxygen charged state ratio has been used as a robust identifier of magnetic clouds (a subset of all interplanetary coronal mass ejections [ICMEs]), when the magnetic field features are not clear enough [*Henke et al.*, 1998], and to establish the coronal sources of the fast and slow wind [*Geiss et al.*, 1995; *von Steiger et al.*, 2001, and references there in].

[16] To separate the slow from the fast streams in the mixed wind, we choose two thresholds. If the charge state ratio of the ionized oxygen (O^{7+}/O^{6+}) goes above an upper threshold, the wind stream is said to be from the hot or slow type, to which we will refer farther in the paper as *slow* stream, and if the charge state ratio is lower than the lower threshold, the wind is fast, coming from the cooler coronal holes and is defined as a *fast* stream. The criterion for choosing the thresholds is that the ion charge state should not cross the value halfway between the two thresholds. This step is necessary to prevent oscillations if the signal wanders around one of the two thresholds.

[17] Additionally, we also use the iron charge state as a criterion to exclude from the analysis periods with CMEs. According to *Lepri and Zurbuchen* [2004] iron charge states equal and greater than 16 are associated with occurrence of CMEs (released from source regions with temperatures around 5 MK).

[18] For the analysis we use 20 seconds averages of magnetic field data of four samples from the ''pure'' fast wind type, four fast streams, seven ''pure'' slow wind and six slow streams. The magnetic field vector data are in the RTN coordinate system, where the R (radial) axis is directed away from the Sun along the sun-spacecraft line, T (tangential) is obtained by the cross-product of the solar rotation axis with the R direction, and N (normal) completes the right-handed system.

4. Results and Discussion

[19] The results of the performed analysis for all periods are summarized also in Table 1. On the basis of the selected examples in Figure 3, in the following subsections we describe the characteristics of the four types of solar wind.

4.1. "Pure" Fast Wind

[20] In Figure 3a the fluctuations of the velocity, density, temperature and magnetic field magnitude are plotted for the example of ''pure'' fast wind (days: 129–133, 1995). The wind speed is high (about 800 km/s), the temperature calculated from the ion composition charge state is about 1 MK and the density is low (about 1 particle in cm^{-3}). The magnetic field magnitude is steady with the well documented ''holes'', associated with the presence of mirror mode structures [*Winterhalter et al.*, 1995]. In general, all the parameters show low variability and relative stationarity with values typical for the high-latitude fast wind.

[21] Figure 4 shows the results of the statistical analysis for this example of ''pure'' fast wind. Figures 4a and 4c represent the power spectral density of the fluctuations with the spectral slope for b_R component and magnetic field magnitude, respectively. The power spectral density is calculated with Welch method by averaging with Hanning window of the Fourier transforms of overlapping samples. The spectral indices are estimated from a linear chi-square fit to the logarithm of the power spectral density versus the logarithm of the frequency. The errors of the fit are given in Table 1. In the radial direction (Figure 4) the fluctuations follow a power law with a slope of −1.65, the famous Kolmogorov index. In the transverse directions (see Table 1), the slope is similar, which means that the turbulence in the pure fast wind is rather homogeneous, as has been already reported in many studies [e.g., *Horbury and Balogh*, 2001; *Horbury et al.*, 1996]. The magnitude how-

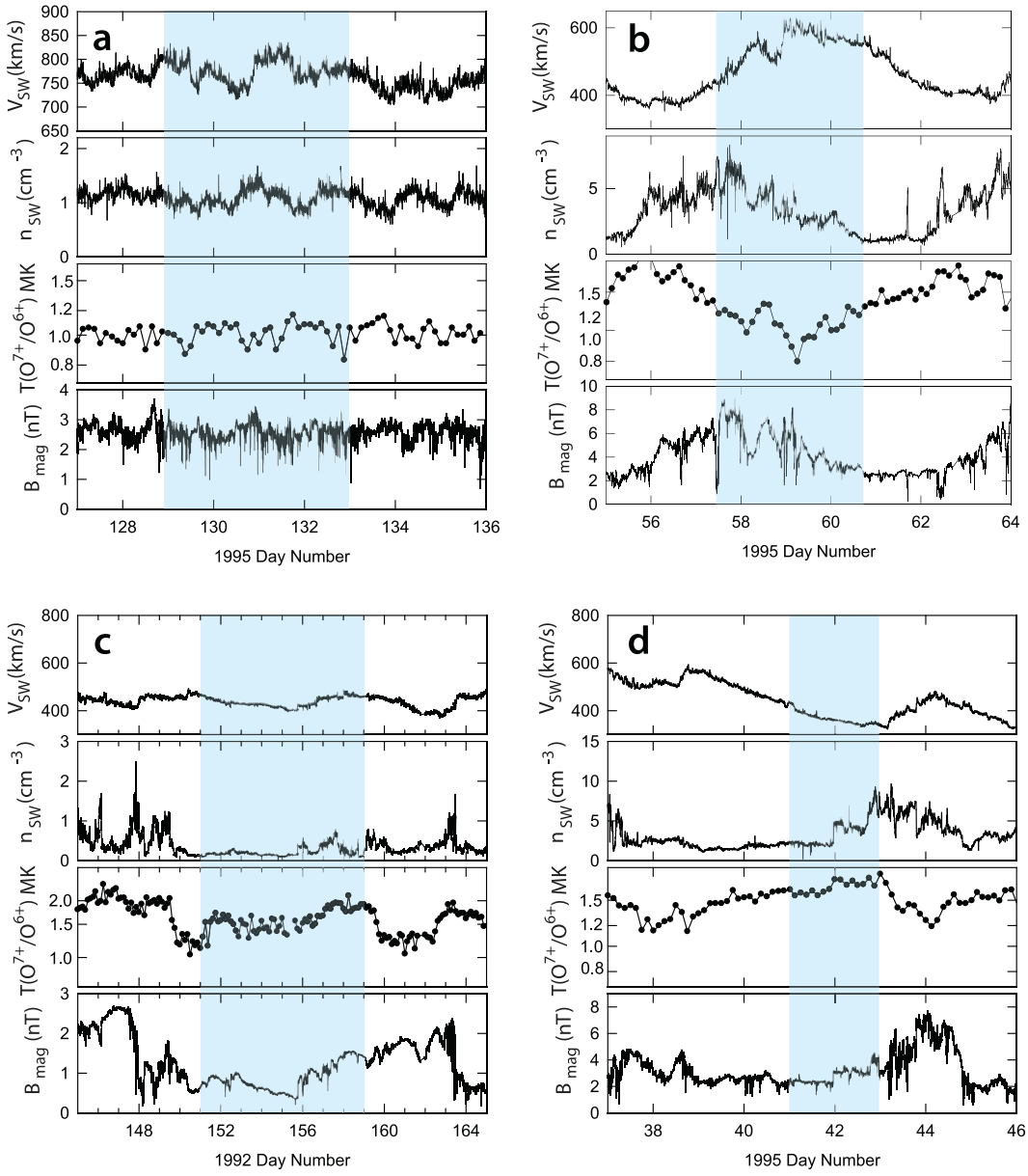

Figure 3. Solar wind fluctuations (from top to bottom: velocity, density, temperature, and magnetic field magnitude) for (a) "pure" fast wind (days: 129–133), (b) fast stream (days: 57.5–60.7), (c) "pure" slow wind (days: 151–159), and (d) slow stream (days: 40.6–43.25).

ever shows slope closer to −1 (Table 1). A similar spectral index was discussed in [*Matthaeus and Goldstein*, 1986; *Bavassano et al.*, 1982b] and was attributed to fluctuations of solar origin. Figure 4b shows the structure function of the b_R magnetic component (b_T and b_N components are not shown for the sake of simplicity of the plot), calculated for powers from 1 to 4 versus the timescales in hours. The inertial range is difficult to define, and is approximately between 10^{-2} and 10^{-1} hours. From a linear fit of the inertial range, the structure function scaling exponents of the three magnetic field components are obtained (Figure 4d, in black). To compare the experimental exponents with the theory we plot as well the linear scaling corresponding to Kolmogorov (fluid) and Kraichnan (magnetofluid) phenomenology (Figure 4d, in red and blue, respectively). The curves of the observed exponents for the three components overlap, confirming the spatial similarity in the fluctuation distribution. They are nonlinear, meaning that in the turbulence there is presence of intermittency.

[22] From the 3-D representation of the fluctuations (as described in section 2.2) we can see how and where in space the magnetic field is distributed. In this particular case, the magnetic field almost entirely fills the different projections (Figures 4e–4h), without showing obvious patches of missing values, meaning that the fluctuations are homogeneously distributed in space. This picture is quite different when compared to the other cases described bellow. The fact, that the b_R component has mainly positive values, corresponds to Ulysses being in unipolar magnetic field along the Parker spiral direction.

[23] Finally, we comment on the flatness (as the quantitative measure of intermittency) for this example (Figure 8a).

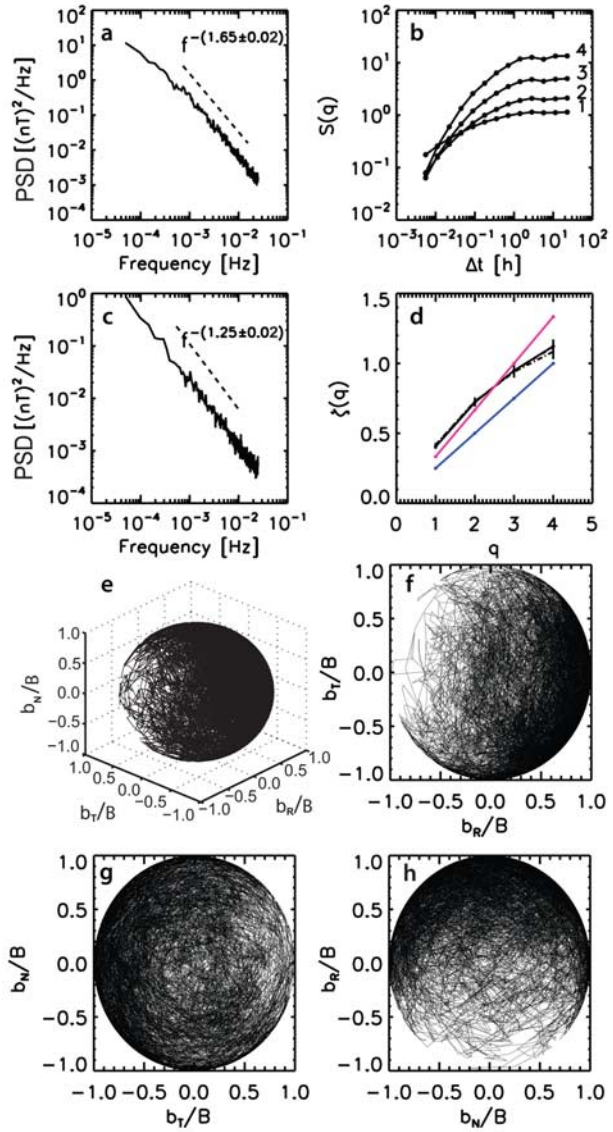

Figure 4. The 1995 "pure" fast wind, days: 129–133. (a) Power spectral density (PSD, solid line) for the b_R component with the respective spectral index (dashed line marks the range of frequency over each the index is determined). (b) Structure function for moments q = [1, 4]. (c) Power spectral density (solid line) for the magnitude with the respective spectral index (dashed line). (d) Structure function exponents with error bars for the three magnetic field components (observations: black solid (b_R), dashed (b_T), and dot-dashed (b_N), and red (Kolmogorov) and blue (Kraichnan) solid lines). (e) 3-D plot of the trajectory of the tip of the magnetic field vector in RTN coordinate system. (f) b_T/B component as a function of b_R/B. (g) b_N/B component as a function of b_T/B. (h) b_R/B component as a function of b_N/B.

The flatness has higher values only for the small timescales (high frequencies) and drops quickly to 3 (the flatness of a Gaussian distribution) at a scale about an hour and a half. *Bruno et al.* [2003] calculated the flatness for the fast wind for different heliospheric distance (0.3–0.9 AU), and at 0.9 AU they obtained about 50% lower value for the flatness than our. They found that the time where the correlation between the scales is lost (flatness equals 3) is three times shorter than our estimation. There is a clear trend in their study for the intermittency to increase with the increase of the distance from the Sun. Considering this evolution and taking into account that our measurements for the discussed period were made at about 1.5 AU, our results confirm the trend.

[24] The power spectra for the other three samples of "pure" fast wind have similar shape and power law: the components show Kolmogorov index and the index for the magnetic field magnitude is closer to −1 (Table 1). However, with the increase of the distance from the Sun, the spectrum for the magnitude of the magnetic field becomes steeper. *Bavassano et al.* [1982b, Table 2] found similar radial evolution in the power spectral slope of the magnitude in distances between 0.29–0.87 AU in approximately the same frequency range (2.8×10^{-4}–10^{-2} Hz).

[25] Two trends can be seen from the flatness values: the higher the heliospheric latitude the higher the intermittency (see, periods 129–133, 165–169, 205–209 of 1995 in Table 1), as well as the larger the distance the higher flatness. For example, the intermittency is high for the period 323–327 of 1995, which is measured both at high heliolatitude (60°N) and large heliocentric distance (3 AU), an effect which is a combinational dependence on both latitude and distance, as mentioned in the introduction. The scales start to be uncorrelated at times in the range from 2 to 8 hours, which is again much larger than what was found by *Bruno et al.* [2003].

4.2. Fast Stream

[26] An example of a measured close to the solar equator fast stream (days: 57.5–60.7, 1995) is shown in Figure 3b. In general, the separated fast streams from the mixed wind show a behavior which is similar in some respects to the "pure" fast wind but different in other respects. The stream speed (top) is lower than that of the "pure" fast wind, showing that the originally fast wind was slowed down in the interaction with a slow stream. The density decreases from a compressed plasma state at the edge with the preceding slow stream to the typical fast wind densities. The oxygen freezing-in temperature decreases as well to about 0.8 MK. The increased magnetic field magnitude close to the beginning of the period also shows sings of compression. All of this emphasizes that in each of the streams of the mixed solar wind there are effects coming from the surrounding streams. There is an interesting feature centered at about day 58.5 in this stream, which resembles an embedded short lasting slow stream, where there is a drop in the solar wind speed, and an increase in the density, temperature and the magnetic field.

[27] The power spectrum of the magnetic field components is close to Kolmogorov (Figure 5a). The spectral index −1.47 of the magnitude is somewhat closer to the MHD (or Kraichnan) power law (Figure 5c). This is an interesting result, since −3/2 slope is usually found to characterize the solar wind velocity and −5/3 slope, the magnetic field [*Podesta et al.*, 2007; *Chapman and Hnat*, 2007]. The amplitude of the fluctuations of the magnitude has a slope also higher than that found for the "pure" fast wind (Table 1). The inertial range seen from the structure

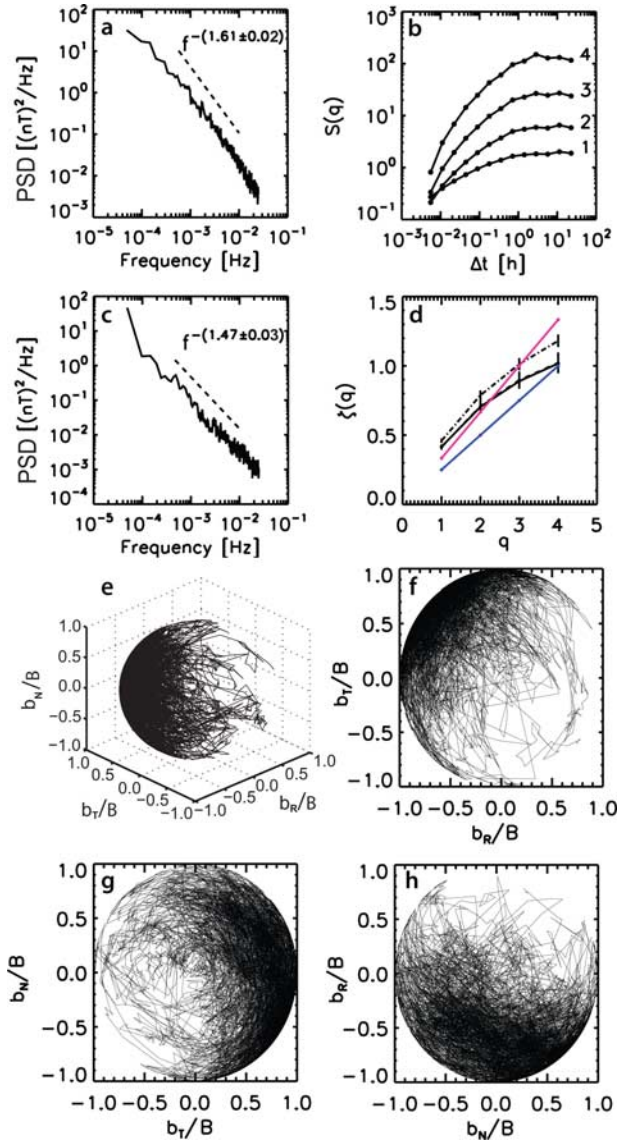

Figure 5. The 1995 fast stream, days: 57.5–60.7. (a–h) Same as in Figure 4.

function is the same as for the "pure" fast wind: 1.10^{-2}–1.10^{-1} hours (Figure 5b). The scaling exponent curves for b_R and b_T components have stronger nonlinearity and smaller values (Figure 5d) than b_N component. The scaling departs from the Kolmogorov and Kraichnan models and shows also a higher intermittency than the "pure" fast wind.

[28] There are denser and rarefied patches in the 3-D plots (Figures 5e–5h), representing the spatial inhomogeneity in the fluctuations. The flatness for the three magnetic field components has similar values (Table 1). The flatness curves (Figure 8b) have the same shape as for the "pure" fast wind (Figure 8a) but the values are almost doubled (Table 1). It takes longer for the fast stream's correlations to be destroyed than those in the "pure" fast wind: from 11 hours in the b_R component to 22 hours for b_T and b_N (Figure 8b). The difference between the characteristics associated with the fast stream and the "pure" fast wind is caused by the compressive effects to which fast solar wind is subjected by the preceding slow stream (the compression seen in the magnetic field in Figure 3b).

[29] The other fast streams were observed at higher heliolatitudes (up to 27°) and larger (up to 4.5 AU) heliocentric distances (Table 1). However, all streams show similar behavior in the power spectra, structure functions, spatial distribution of the fluctuations and flatness values to the above shown example. The only significant difference between the streams is that the timescales become uncorrelated at different times; from several hours for days (304–315 of 1996) up to couple of days in the period (47.5–49.5 of 1995).

4.3. "Pure" Slow Wind

[30] The measurements of the "pure" slow wind were made within several degrees of the solar equator and at large heliocentric distances (Table 1). From the example given in Figure 3c, it is seen that this type of wind is characterized by low speed, density and magnetic field. In contract to the "pure" fast wind and fast streams, it is much hotter, with oxygen freezing-in temperature for this particular period about 1.7 MK, which reflects the fact that the slow wind originates from the active coronal regions.

[31] The power spectral index for both magnetic field components and magnitude is similar to Kolmogorov (Figures 6a and 6c). In difference to the "pure" fast wind and fast streams, the magnitude's spectrum is steeper. Interestingly, the inertial range determined from the structure function (Figure 6b) is the same as for the fast wind and fast streams: 1.10^{-2}–1.10^{-1} hours (taking into account a correction for the shift toward larger scales caused by the measurements in the spacecraft frame). The scaling exponents for b_R and b_N components show stronger nonlinearity and deviation from the Kolmogorov scaling than the b_T component.

[32] There is an obvious contrast in the spatial distribution of the fluctuations between "pure" slow wind and "pure" fast wind and fast streams. There are big rarefied even empty patches in the fluctuations, especially for the b_T component and to a lesser extent for the b_R component. This poor space-filling appearance is well seen in Figure 6e, as well as in the projections containing b_T and b_R components. The concentration of the magnetic field vector in two opposite values of b_T could be an indication for a sector boundary in this particular case.

[33] The flatness curves (Figure 8c) and flatness values (Table 1) show that b_T is the most intermittent component, followed by b_R and b_N component, which is the least intermittent one. The flatness becomes Gaussian at a timescale about 11 hours for b_R component, 34 hours for b_T and 17 hours for b_N (Figure 8c). *Bruno et al.* [2003] found that at 0.9 AU the slow wind becomes Gaussian at a timescale of about 3 hours.

[34] There are no common trends in the behavior of the "pure" slow wind periods. The power spectrum and intermittency show great variability independent of the latitude and distance from the Sun. For the components the spectral index ranges from −1.45 to −1.83, and for the magnitude from −1.55 to −1.76 (Table 1). Similar ranges of spectral slopes for the slow wind have been reported by *Bruno et al.* [2007b]. The flatness values although widely spread are in general higher than in the fast solar wind, meaning that the

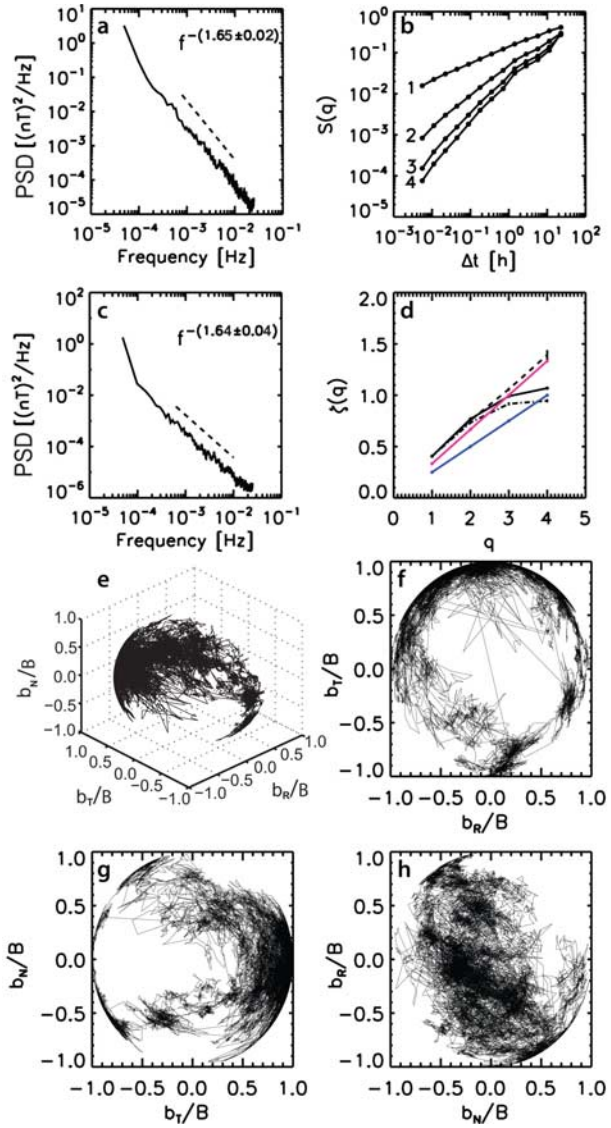

Figure 6. The 1995 "pure" slow wind, days: 151–159. (a–h) Same as in Figure 4.

intermittency for the "pure" slow wind is more prominent. There are periods in which the strongest intermittency is estimated for the b_T component. Interestingly, these periods contain shocks or they are in the vicinity of shocks or CMEs. This apparently large and systematic asymmetry in the behavior of the components may be caused by a preferential alignment of discontinuity normals [*Siscoe et al.*, 1968; *Knetter et al.*, 2004; *Erdős and Balogh*, 2008]. As the intervals analyzed necessarily contain many discontinuities, these may well differentially affect the intermittency in the components. The stronger intermittency is suggested to reflect the presence of sharp gradients of the wind within its stochastic fluctuations [*Bruno and Carbone*, 2005]. These large gradients are characteristic of the slow solar wind, especially during high solar activity. The net effect of their presence is that of increased intermittency which, in turn, makes the behavior more similar to that of a passive scalar advected by ordinary turbulence [*Bruno et al.*, 2007a].

4.4. Slow Stream

[35] An example of a slow stream is presented in Figure 3d. Typically this type of wind is much denser than the "pure" slow wind and both "pure" fast wind and fast streams. The speed of the stream is slightly lower, 390 km/s on average (Figure 3d, top) than the speed of the "pure" slow wind, which is about 440 km/s (Figure 3c). The slow stream is as hot as the "pure" slow wind, about 1.7 MK coronal temperature (Figure 3d), since both types of wind originate from the same sources in the corona. The density steadily increases toward the stream edge with the neighboring fast stream. This compression is also well seen in the magnetic field magnitude (Figure 3d).

[36] The spectral index for both the magnetic field components and magnitude (~ -1.73 and -1.78, Figures 7a and 7c, respectively; also Table 1) is steeper than the Kolmogorov slope. The inertial range (Figure 7b) is also the same as for the other types of wind described in the sections

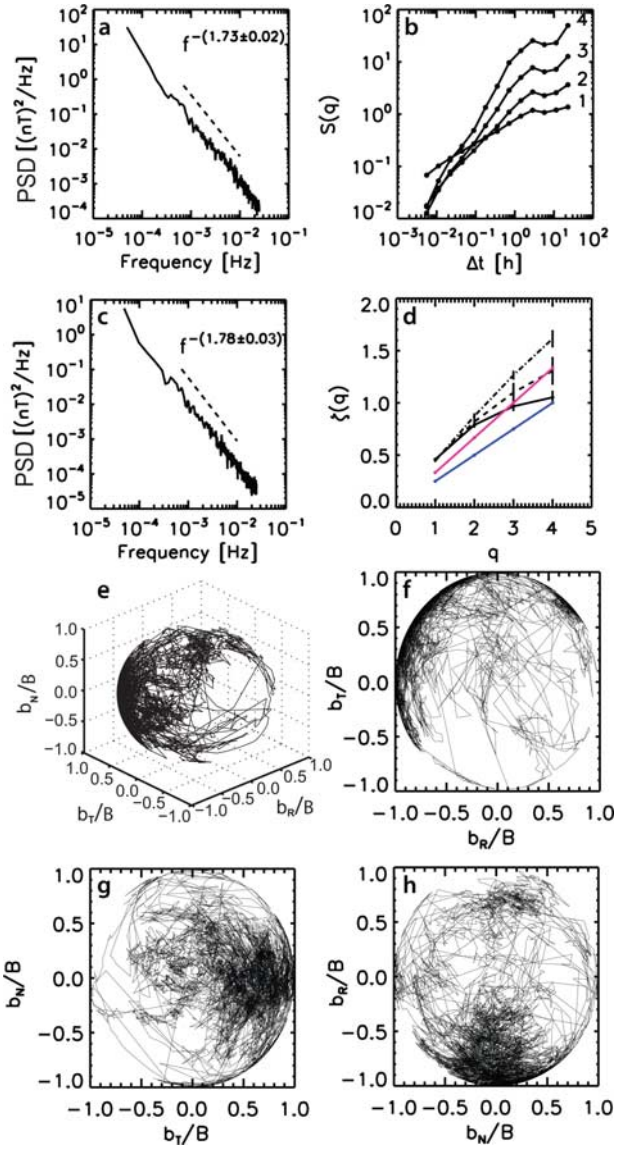

Figure 7. The 1995 slow stream, days: 40.6–43.25. (a–h) Same as in Figure 4.

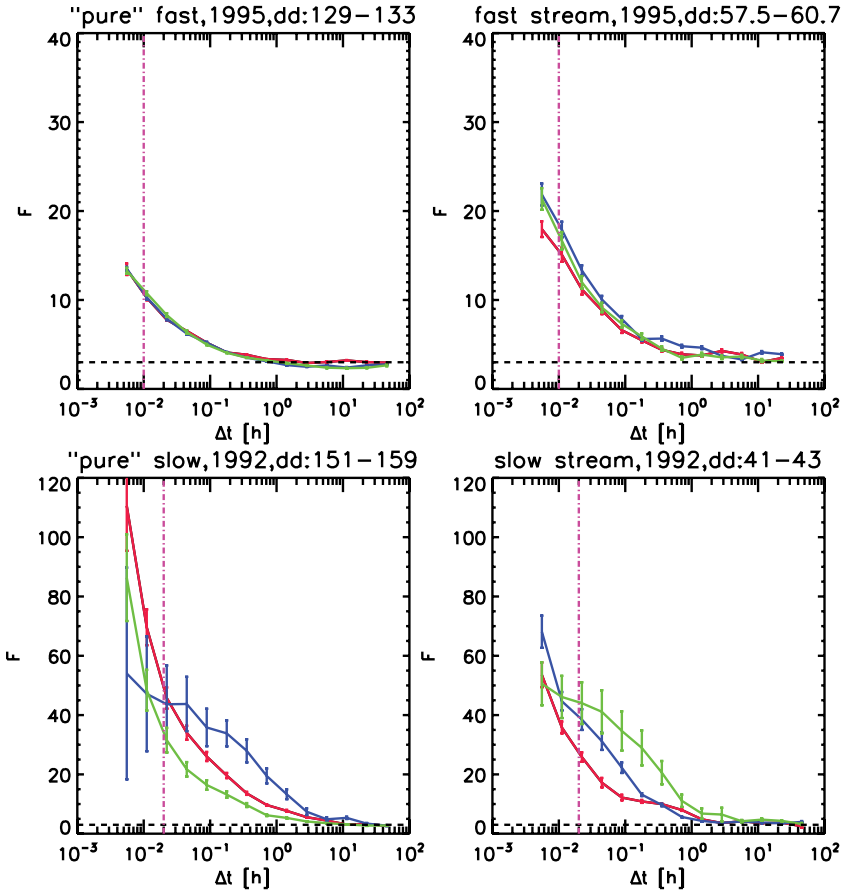

Figure 8. Flatness for (a) "pure" fast wind (days: 129–133), (b) fast stream (days: 57.5–60.7), (c) "pure" slow wind (days: 151–159), and (d) slow stream (days: 40.6–43.25). The b_R component is shown in red, b_T in blue, and b_N in green with error bars for each flatness value. The vertical magenta dash-dotted lines mark the timescale chosen for the flatness comparison discussed in the text (flatness values are given in Table 1), and the horizontal black dashed line marks the value of the flatness (F = 3) for a Gaussian distribution.

above. The scaling exponent of b_R component shows strongest nonlinearity and b_N (the weakest) (Figure 7d). All three components deviate from the theoretical models for neutral and magneto-fluid turbulence.

[37] The spatial distribution of the fluctuations is very inhomogeneous (Figures 7e–7h). The most rarefied are the distributions related to b_T and b_N components. These are also the components mostly affected by intermittency (Table 1); the highest flatness is observed for b_N and the least intermittent is b_R (Figure 8d). Given the time range of the measurements, the time where the correlations between the scales are destroyed cannot be reached.

[38] Similarly to the "pure" slow wind, the slow streams separated from the mixed wind in the equatorial region (up to 22°) do not have common trends. The power spectral slopes for the components and the magnitude (Table 1) have similar variable behavior as for the "pure" slow wind. On the other hand, the intermittency in the slow streams is lower than the one found for the "pure" slow wind. Summarizing the results for all slow streams (Table 1), it becomes clear that neither the spectrum nor the intermittency level show any dependence on heliolatitude and distance. The lack of such dependence was also found in the work of *Bruno et al.* [2003] for the slow wind observed in the ecliptic plane. However, it is very interesting to note that their estimation for the flatness at 0.9 AU is much smaller than our results for heliocentric distances ranging from 1.4–5 AU. The time on which the scales become uncorrelated also varies to a great extent: from about 22 hours (days: 134–138, 1997) to about 4 days (days: 320–325, 1996), being much larger than the 3 hours estimated in the study of *Bruno et al.* [2003].

5. Conclusions

[39] This paper presents a new/detailed look at the complex solar wind turbulence. The magnetic field turbulence shows different properties dependent on the coronal source regions, heliolatitude, heliocentric distance and level of solar activity. Because of this complicated behavior we classify solar wind in different types, in order to investigate the turbulence properties as a function of its region of origin in the corona and the dynamic context of the different

streams. We have confirmed some known trends and established new ones.

5.1. Turbulence Nature

[40] The nature of turbulence in the different solar wind types is different, because of the different region of origin in the corona, where kinetic differentials are not the dominant features. The fact that in the "pure" slow wind, the structure and kinetics are very variable, would affect the dynamics, which in turn will affect the turbulence. In the slow wind we do not see spectral slope of -1, meaning that the solar wind leaving the corona is already multiscale, composed of waves and convected structures, which interact locally and therefore the dynamics going to be other than Kolmogorov. In difference, the absence of velocity shears in the fast wind cause slower turbulence evolution. The differentiation in the solar wind types is well seen from the power spectrum of the magnetic field magnitude: the "pure" fast has a slope ~ -1.33 ($1/f$-like), the fast streams has ~ -1.48 (Kraichnan-like), the "pure" slow wind has ~ -1.67 (Kolmogorov-like) and the slow streams has ~ -1.72.

5.2. Intermittency

[41] Regardlessly of the type of the solar wind, the turbulence in general is intermittent. Because of the lack of dynamical interactions (compressions, velocity shears) between streams with different speeds, the "pure" fast wind in the polar heliolatitudes is less intermittent than the others: "pure" slow wind, and both slow and fast streams. In the equatorial plane, the separation of the interacting streams revealed that the fast streams are less intermittent than the slow streams. This distinct behavior shows that the solar wind turbulence cannot be treated without reference to its region of origin and the dynamic context [*Horbury et al.*, 1996; *Bruno and Carbone*, 2005]. Even though separated we still could see that the intermittency level in the different streams is affected by compressional processes and velocity shears, i.e., fast streams are more intermittent than the "pure" fast wind, and slow streams are less intermittent than the "pure" slow winds. The timescales for the different solar wind types at which they become uncorrelated are also widely various: from several hours for the "pure" fast wind, through couple of days for the fast streams and "pure" slow wind, up to 4 days for the slow streams.

5.3. Radial Evolution

[42] The spectral properties of the magnetic field magnitude of the "pure" fast wind evolve in radial direction toward a more MHD-like turbulence [*Tu and Marsch*, 1995; *Goldstein et al.*, 1995; *Matthaeus et al.*, 1995; *Horbury et al.*, 1996]. The "pure" fast wind is also the only type of wind which intermittency shows clear radial and latitudinal evolution. The fast streams, the "pure" slow wind and the slow streams, all of them in the equatorial plane do not show evolution either in heliolatitude, or in heliocentric distance over the analyzed range (1.4–5.4 AU). However, we note that our flatness estimations as a function of the distance from the Sun beyond 0.9 AU of previous estimations [*Bruno et al.*, 2003], are much higher. A clear radial dependence of nonpropagating magnetically dominated structures advected with the solar wind expansion, was also found within the fast wind, but not within the slow wind [*Bruno et al.*, 2007c].

5.4. Solar Activity

[43] We note that our results cover periods of solar activity away from maximum. Around solar maximum, there are no longer coronal holes and there are only short-lived fast wind streams at all heliolatitudes. As a result, no "pure" fast solar wind, as we have defined in this paper, can be observed. The heliospheric medium is dominated by a mix of CMEs and short-lived interaction regions [*Balogh and Smith*, 2001; *Gosling et al.*, 2001]. Despite the presence of the occasional high-speed stream, we expect that the turbulence properties of the solar wind may be close to those we have derived for the slow streams and "pure" slow wind.

[44] **Acknowledgments.** The authors would like to thank G. Erdõs, R. J. Forsyth, A. P. Rossi, and Z. Vörös for their help in preparing this manuscript.

[45] Amitava Bhattacharjee thanks Eckart Marsch and another reviewer for their assistance in evaluating this paper.

References

Balogh, A., and E. J. Smith (2001), The heliospheric magnetic field at solar maximum: Ulysses observations, *Space Sci. Rev.*, *97*, 147–160, doi:10.1023/A:1011854901760.

Balogh, A, T. J. Beek, R. J. Forsyth, P. C. Hedgecock, R. J. Marquedant, E. J. Smith, D. J. Southwood, and B. T. Tsurutani (1992), The magnetic field investigation on the ULYSSES mission: Instrumentation and preliminary scientific results, *Astron. Astrophys. Suppl. Ser.*, *92*, 221–236.

Balogh, A., J. T. Gosling, J. R. Jokipii, R. Kallenbach, and H. Kunow (1999), Introduction, *Space Sci. Rev.*, *89*, 1–3, doi:10.1023/A:1005203608266.

Bavassano, B., M. Dobrowolny, G. Fanfoni, F. Mariani, and N. F. Ness (1982a), Statistical properties of MHD fluctuations associated with high-speed streams from Helios-2 observations, *Sol. Phys.*, *78*, 373–384.

Bavassano, B., M. Dobrowolny, F. Mariani, and N. F. Ness (1982b), Radial evolution of power spectra of interplanetary Alfvénic turbulence, *J. Geophys. Res.*, *87*, 3616–3622.

Bavassano, B., R. Bruno, and R. D'Amicis (2009), Velocity fluctuations in polar solar wind: A comparison between different solar cycles, *Ann. Geophys.*, *27*, 877–883.

Belcher, J. W., and L. Davis Jr. (1971), Large-amplitude Alfvén waves in the interplanetary medium: 2, *J. Geophys. Res.*, *76*, 3534–3563.

Bruno, R., and V. Carbone (2005), The solar wind as a turbulence laboratory, *Living Rev. Sol. Phys.*, *2*(4), 1–186.

Bruno, R., V. Carbone, L. Sorriso-Valvo, and B. Bavassano (2003), Radial evolution of solar wind intermittency in the inner heliosphere, *J. Geophys. Res.*, *108*(A3), 1130, doi:10.1029/2002JA009615.

Bruno, R., V. Carbone, S. Chapman, B. Hnat, A. Noullez, and L. Sorriso-Valvo (2007a), Intermittent character of interplanetary magnetic field fluctuations, *Phys. Plasmas*, *14*(3), 032901, doi:10.1063/1.2711429.

Bruno, R., R. D'Amicis, B. Bavassano, V. Carbone, and L. Sorriso-Valvo (2007b), Scaling laws and coherent structures in the solar wind, *Planet. Space Sci.*, *55*, 2233–2238, doi:10.1016/j.pss.2007.05.005.

Bruno, R., R. D'Amicis, B. Bavassano, V. Carbone, and L. Sorriso-Valvo (2007c), Magnetically dominated structures as an important component of the solar wind turbulence, *Ann. Geophys.*, *25*, 1913–1927.

Burlaga, L. F. (1991), Intermittent turbulence in the solar wind, *J. Geophys. Res.*, *96*, 5847–5851.

Chapman, S. C., and B. Hnat (2007), Quantifying scaling in the velocity field of the anisotropic turbulent solar wind, *Geophys. Res. Lett.*, *34*, L17103, doi:10.1029/2007GL030518.

Chapman, S. C., B. Hnat, and K. Kiyani (2008), Solar cycle dependence of scaling in solar wind fluctuations, *Nonlinear Process. Geophys.*, *15*, 445–455.

Coleman, P. J., Jr. (1968), Turbulence, viscosity, and dissipation in the solar-wind plasma, *Astrophys. J.*, *153*, 371–388.

Denskat, K. U., and F. M. Neubauer (1982), Statistical properties of low-frequency magnetic field fluctuations in the solar wind from 0.29 to 1.0 AU during solar minimum conditions: HELIOS 1 and HELIOS 2, *J. Geophys. Res.*, *87*, 2215–2223.

Erdős, G., and A. Balogh (2008), Density of discontinuities in the heliosphere, *Adv. Space Res.*, *41*, 287–296, doi:10.1016/j.asr.2007.04.036.

Forsyth, R. J., T. S. Horbury, A. Balogh, and E. J. Smith (1996), Hourly variances of fluctuations in the heliospheric magnetic field out of the ecliptic plane, *Geophys. Res. Lett.*, *23*, 595–598.

Frisch, U. (1995), *Turbulence: The Legacy of A.N. Kolmogorov*, Cambridge Univ. Press, New York.

Geiss, J., G. Gloeckler, and R. von Steiger (1995), Origin of the solar wind from composition data, *Space Sci. Rev.*, *72*, 49–60, doi:10.1007/BF00768753.

Goldstein, M. L., and D. A. Roberts (1999), Magnetohydrodynamic turbulence in the solar wind., *Phys. Plasmas*, *6*, 4154–4160.

Goldstein, M. L., D. A. Roberts, and W. H. Matthaeus (1995), Magnetohydrodynamic turbulence in the solar wind, *Annu. Rev. Astron. Astrophys.*, *33*, 283–326, doi:10.1146/annurev.aa.33.090195.001435.

Gosling, J. T., D. J. McComas, R. M. Skoug, and R. J. Forsyth (2001), Stream interaction regions at high heliographic latitudes during Ulysses12/22/2004 6:25PM second polar orbit, *Space Sci. Rev.*, *97*, 189–192, doi:10.1023/A:1011871421324.

Henke, T., et al. (1998), Differences in the O^{7+}/O^{6+} ratio of magnetic cloud and non-cloud coronal mass ejections, *Geophys. Res. Lett.*, *25*, 3465–3468.

Horbury, T. S., and A. Balogh (1997), Structure function measurements of the intermittent mhd turbulent cascade, *Nonlinear Process. Geophys.*, *4*, 185–199.

Horbury, T. S., and A. Balogh (2001), Evolution of magnetic field fluctuations in high-speed solar wind streams: Ulysses and Helios observations, *J. Geophys. Res.*, *106*, 15,929–15,940.

Horbury, T. S., A. Balogh, R. J. Forsyth, and E. J. Smith (1996), The rate of turbulent evolution over the Sun's poles, *Astron. Astrophys.*, *316*, 333–341.

Kiyani, K., S. C. Chapman, B. Hnat, and R. M. Nicol (2007), Self-similar signature of the active solar corona within the inertial range of solar-wind turbulence, *Phys. Rev. Lett.*, *98*(21), 211101, doi:10.1103/PhysRevLett.98.211101.

Knetter, T., F. M. Neubauer, T. Horbury, and A. Balogh (2004), Four-point discontinuity observations using Cluster magnetic field data: A statistical survey, *J. Geophys. Res.*, *109*, A06102, doi:10.1029/2003JA010099.

Lepri, S. T., and T. H. Zurbuchen (2004), Iron charge state distributions as an indicator of hot ICMEs: Possible sources and temporal and spatial variations during solar maximum, *J. Geophys. Res.*, *109*, A01112, doi:10.1029/2003JA009954.

Marsch, E., and C.-Y. Tu (1990), On the radial evolution of MHD turbulence in the inner heliosphere, *J. Geophys. Res.*, *95*, 8211–8229.

Marsch, E., and S. Liu (1993), Structure functions and intermittency of velocity fluctuations in the inner solar wind, *Ann. Geophys.*, *11*, 227–238.

Matthaeus, W. H., and M. L. Goldstein (1986), Low-frequency 1/f noise in the interplanetary magnetic field, *Phys. Rev. Lett.*, *57*, 495–498.

Matthaeus, W. H., J. W. Bieber, and G. P. Zank (1995), Unquiet on any front: Anisotropic turbulence in the solar wind, *Rev. Geophys.*, *33*, 609–614.

Podesta, J. J., D. A. Roberts, and M. L. Goldstein (2007), Spectral exponents of kinetic and magnetic energy spectra in solar wind turbulence, *Astrophys. J.*, *664*, 543–548, doi:10.1086/519211.

Roberts, D. A, and M. L. Goldstein (1991), Turbulence and waves in the solar wind, *Rev. Geophys.*, *29*, 932–943.

Roberts, D. A., M. L. Goldstein, L. W. Klein, and W. H. Matthaeus (1987), Origin and evolution of fluctuations in the solar wind: HELIOS observations and Helios-Voyager comparisons, *J. Geophys. Res.*, *92*, 12,023–12,035.

Siscoe, G. L., L. Davis Jr., P. J. Coleman Jr., E. J. Smith, and D. E. Jones (1968), Power spectra and discontinuities of the interplanetary magnetic field: Mariner 4, *J. Geophys. Res.*, *73*, 61–62.

Tu, C.-Y., and E. Marsch (1995), MHD structures, waves and turbulence in the solar wind: Observations and theories, *Space Sci. Rev.*, *73*, 1–2.

von Steiger, R., T. H. Zurbuchen, J. Geiss, G. Gloeckler, L. A. Fisk, and N. A. Schwadron (2001), The 3-D heliosphere from the Ulysses and ACE solar wind ion composition experiments, *Space Sci. Rev.*, *97*, 123–127, doi:10.1023/A:1011886414964.

Wimmer-Schweingruber, R. F., R. von Steiger, and R. Paerli (1997), Solar wind stream interfaces in corotating interaction regions: SWICS/Ulysses results, *J. Geophys. Res.*, *102*, 17,407–17,417.

Winterhalter, D., M. Neugebauer, B. E. Goldstein, E. J. Smith, B. T. Tsurutani, S. J. Bame, and A. Balogh (1995), Magnetic holes in the solar wind and their relation to mirror mode structures, *Space Sci. Rev.*, *72*, 201–204, doi:10.1007/BF00768780.

A. Balogh and R. von Steiger, International Space Science Institute, Hallerstrasse 6, CH-3012, Bern, Switzerland.

A. Noullez, Laboratoire Casioppe, Observatoire de la Côte d'Azur, B. P. 4229, F-06304 Nice Cedex 4, France.

E. Yordanova, Space Plasma Physics, Swedish Institute of Space Physics, Box 537, SE-751 21 Uppsala, Sweden. (eya@irfu.se)